Theor Chim Acta (1987) 71: 201-229

Theoretica Chimica Acta



# Exponentially generated wave functions and excited states of benzene

**Hiroshi Nakatsuji**

Division of Molecular Engineering, Graduate School of Engineering, Kyoto University, Kyoto 606, Japan

(Received September 1 / Accepted September 29, 1986)

Usefulness of the exponentially generated wave function approach is shown. We first give an overview of the SAC (symmetry adapted cluster) and SAC-CI study on the valence and Rydberg excitations and ionizations of benzene including both $\pi$ and $\sigma$ spaces. The importance of the $\sigma$ reorganization effect is found for the $T_3(^3B_{2u})$, $S_2(^1B_{1u})$, and $S_3(^1E_{1u})$ states, so-called V states. A first systematic calculation is reported for the Rydberg excited states. Next, the idea of the exponentially generated wave function (EGWF) theory is explained. New exponential-type operators and new wave functions associated with them are defined. The mixed or multi use of these exponential operators is shown to be effective both physically and practically. We call the resultant wave functions MEG (multi-exponentially generated) wave functions. We then explain the algorithm of calculations and show some results on the potential energy curves of the ground, excited, and quasi-degenerate states of some diatomics and triatomics.

**Key words:** Exponentially generated wave function — Cluster expansion — SAC-CI — Excited state — Benzene

## 1. Introduction

In recent years, the needs for accurate theories of molecular excited states are more and more increasing. This trend is partially due to a demand from active experimental developments in molecular spectroscopy such as in laser chemistry and in synchrotron orbital radiation chemistry. We have been engaged for almost ten years in the quantum chemistry of molecular excited states. The purpose has

been to develop accurate and useful theories of molecular excited states. The theory of molecular excited states may be grouped into two stages: one is the theory for molecular spectroscopy near vertically excited states, and the other is the theory useful for studying dynamics and chemical reactions involving molecular excited states. For the latter purpose, we need accurate knowledge of the potential energy surfaces and the properties involving ground state and several excited states.

Our approach to the theory of excited states is as follows. Near vertical excitations, we use SAC (symmetry adapted cluster) expansion theory [1] to calculate ground states, and SAC-CI theory [2, 3] to study excited, ionized, and anion states. To calculate wave functions and energies for all possible nuclear configurations, the SAC theory, which is a Hartree-Fock reference theory, sometimes breaks down. We therefore consider the multireference version of the SAC theory, called MR-SAC theory [4], and the exponentially generated wave function (EGWF) theory [5], which is more general than the MR-SAC theory. In this symposium, we first explain briefly the SAC and SAC-CI approach giving some recent results on the excited states of benzene [6]. Then, we explain our recent EGWF approach and give some progress report of the applications of this theory.

## 2. SAC and SAC-CI theory

The Ursell-Meyer exponential cluster expansion ansatz was first introduced for a closed-shell ground state by Coester and Kümmel [7] and later introduced and applied successfully in the field of quantum chemistry by Sinanoglu [8], Primas [9], Cizek and Paldus [10], Mukherjee et al. [11] and Bartlett [12]. The SAC expansion [1] belongs to this approach and is a generalization to open-shell systems. In the SAC expansion, we operate the exponential of the symmetry adapted excitation operator $S_I^\dagger$ to the Hartree-Fock (HF) function $|0\rangle$.

$$\Psi^{\mathrm{SAC}} = \mathcal{O} \exp\left(\sum_I C_I S_I^\dagger\right)|0\rangle. \tag{1}$$

Here, the symmetry adaptation of the operator is necessary because of a non-linear nature of the expansion. The operator $\mathcal{O}$ is a symmetry projector, but it is unnecessary for totally symmetric systems. This expansion is suitable for both closed- and open-shell molecules, and describes self-consistency [13] and dynamic correlations [8] very well. We formulated the SAC theory in both variational [1] and non-variational [3] frameworks.

We showed [1] that the SAC expansion is different from the conventional coupled cluster expansion [10] especially for open-shell systems. Though the conventional expansions have some difficulties [1] for open-shell systems, the SAC expansion does not have. In the limit that we include only single excitations in the excitation operators, the ordinary cluster expansion reduces to the UHF (unrestricted HF) wave function as Thouless' theorem implies [1, 13]. It is not an eigenfunction of the spin-squared operator and has some other defects [14]. On the other hand, the SAC theory reduces, in the same limit, to the pseudo-orbital theory as we already showed [1, 15].

Two roles of the SAC theory are important. One is to give an accurate wave function to the ground state. The other is to give, at the same time, a subspace of the functions which are orthogonal and hamiltonian-orthogonal to the SAC wave function. Such functions are defined by

$$\Phi_K = \mathscr{P} R_K^\dagger \Psi^{\mathrm{SAC}}, \tag{2}$$

where $R_K^\dagger$ is a symmetry-adapted excitation operator and $\mathscr{P}$ projects out the SAC function. The functions $\{\Phi_K\}$ satisfy [2]

$$\langle \Phi_K | \Psi^{\mathrm{SAC}} \rangle = 0, \qquad \langle \Phi_K | H | \Psi^{\mathrm{SAC}} \rangle = 0. \tag{3}$$

This relation is a necessary condition which the excited state should satisfy. The functions $\{\Phi_K\}$ thus span the space for the excited state. Therefore, we describe the excited state by a linear combination of these functions

$$\Psi^{\mathrm{SAC\text{-}CI}} = \sum_K d_K \Phi_K \tag{4}$$

which is the SAC-CI wave function [2].

We use the SAC-CI theory to describe excited states, ionized states, and electron attached states. For the latter two cases, the operator $R_K^\dagger$ in Eq. (2) is an ionization or electron attachment operator, respectively. The condition expressed by Eq. (3) is automatically satisfied in these cases. The SAC-CI theory is more rapidly convergent than an ordinary CI because it satisfies the necessary condition for the excited states (Eq. (3)), and because it starts from the ground state correlation as seen from Eq. (2). The primary processes of excitations and ionizations involve only one or two electrons and the other electrons lie in the situation similar to that in the ground state. It is, therefore, a better approximation of the excited or ionized states to describe them based on the ground state correlated wave functions, as in Eq. (2), rather than to describe the excited-state correlations from the first beginning as in the CI theory. In a previous paper [3], we described both variational and non-variational solutions of the SAC-CI theory.

The SAC and SAC-CI theory have been applied successfully to the excited and ionized states of $H_2O$ [3, 16, 17], $CH_2$ [18], $H_2CO$ [19], $CO_2$, $N_2O$ [20], NO radical [21], glyoxal [22], ethylene [23], $NH_4^+$ [24], pyrrole, furan, and cyclopentadiene [25], and to the potential energy curves of the ground and excited states of $Li_2$ [26], CO [27], $PdH_2$, and $Pd_2H_2$ [28] molecules. The last two systems are studied as a model of the dissociative adsorption of a hydrogen molecule on a palladium surface. We have studied the one- and two-electron processes in the ionization spectra of $H_2O$ [29], $CO_2$, $N_2O$ [20], $CS_2$, COS [30], NO radical [21] and benzene [31]. We have also studied spin- and electron-correlation effects on the hyperfine splitting constants of several open-shell radicals [15, 32–34].

The program system for the SAC and SAC-CI calculations have been published [35]. It can deal with singlet closed shell ground state by the SAC theory and singlet and triplet excited states, doublet ionized and electron attached states by the SAC-CI theory. The basic algorithms used in this program were explained previously [3, 20].

### 3. Excited states and ionized states of benzene

We apply here the SAC and SAC-CI theory to the valence and Rydberg excitations and ionizations of benzene. Benzene is a key aromatic molecule and is probably one of the best studied molecules like ethylene. This molecule is also a historical molecule in the development of molecular quantum chemistry. It was a central molecule in the Hückel $\pi$-electron theory [36] and in the Pauling's resonance theory [37]. This idea was further developed by Goeppart-Mayer and Sklar [38], Pariser, Parr [39] and Pople [40] as the $\pi$-electron theory of conjugated hydrocarbons. However, *ab initio* study of the excited states of benzene is still very limited [41-46]. The most thorough study is probably due to Hay and Shavitt [45], but this is still limited to within $\pi$-electron CI. Only the lower three states, two triplets and one singlet, were described rather reasonably by the *ab initio* $\pi$-electron CI theories, if they include more than triple excitations.

The calculational details are as follows. We use the experimental geometry of the ground state [47] for all the states. We use three kinds of basis set. The basis $\#0$ is the one used by Hay and Shavitt [45], double zeta Huzinaga-Dunning set [48] plus Rydberg $p_\pi$ orbitals on each carbon. For the valence excitations, we further add to basis $\#0$ the $d_\pi$ polarization functions on each carbon ($\zeta_d = 0.75$) [49]. This is basis set $\#1$. For the calculations of the Rydberg excitations, we add to the basis $\#0$ the $s$, $p$, and $d$ functions in double $\zeta$ accuracy at the center of the molecule ($\zeta_s = 0.0184, 0.0437$; $\zeta_p = 0.0168, 0.0399$; $\zeta_d = 0.0120, 0.0285$) [49]. This is basis set $\#2$. The active space consists of all $\pi$ MO's and almost all $\sigma$ MO's, namely 80 MO's. The dimension of the calculation becomes relatively small by virtue of the SAC-CI theory. In the present algorithm, the dimension becomes to that of the SD (singles and doubles) CI though the calculation includes up to the quadruple excitations in the unlinked approximation. Further, by adopting the configuration selection scheme [20], we can choose an optimal dimension of the calculation, even if we use a large active space. Because of this merit we can include even the $\sigma$-electron space. The dimensions adopted here are less than 4 thousands. For integral transformation, we use the Bender algorithm [50] and for sorting the Yoshimine algorithm [51]. The SCF calculation is performed by HONDOG program [52] and the SAC/SAC-CI calculation is performed with a slightly modified version of the SAC85 program [35].

The Hartree-Fock energy of benzene calculated with the basis $\#1$ is $-230.660466$ a.u. The correlation energy of the ground state is calculated to be $-0.08771$ a.u. by the SAC theory when only the $\pi$ space ($35\pi$ MO's) is considered. When the $\sigma$ space is included ($35\pi + 45\sigma$), the correlation energy becomes $-0.19764$ a.u., more than twice as large as that of the $\pi$ space only.

Table 1 shows the results for the valence $\pi \rightarrow \pi^*$ excitations of benzene. It compares with experiments [53], the SDT $\pi$-CI results of Hay and Shavitt [45], the $35\pi$ SAC-CI results, and the $35\pi + 45\sigma$ SAC-CI results. The values in parentheses show the deviations from the experimental values. We call the $\pi \rightarrow \pi^*$ excitations to the $^1B_{2u}$, $^1B_{1u}$ and $^1E_{1u}$ states as $S_1$, $S_2$ and $S_3$ states, respectively,

**Table 1.** Valence $\pi \rightarrow \pi^*$ excitation energy of benzene (eV)[a]

| State | SDT $\pi$-CI[b] Hay-Shavitt[b] $23\pi$ | SAC-CI[c] $35\pi$ | SAC-CI[c] $35\pi+45\sigma$ | Exptl.[d] |
|---|---|---|---|---|
| $^1B_{2u}(S_1)$ | 5.00 (0.10) | 5.25 (0.35) | 5.25 (0.35) | 4.90 |
| $^1B_{1u}(S_2)$ | 7.64 (1.44) | 7.31 (1.11) | 6.60 (0.40) | 6.20 |
| $^1E_{1u}(S_3)$ | 8.34 (1.39) | 8.25 (1.30) | 7.47 (0.52) | 6.95 |
| $^3B_{1u}(T_1)$ | 3.83 (−0.12) | 3.80 (−0.15) | 4.06 (0.11) | 3.95 |
| $^3E_{1u}(T_2)$ | 4.98 (0.23) | 5.05 (0.30) | 5.02 (0.27) | 4.75 |
| $^3B_{2u}(T_3)$ | 7.00 (1.40) | 6.65 (1.05) | 6.02 (0.42) | 5.60 |

[a] Values in parentheses show the deviations from the experimental values
[b] Basis set #0
[c] Basis set #1
[d] [53]

and to the $^3B_{1u}$, $^3E_{1u}$ and $^3B_{2u}$ states as $T_1$, $T_2$ and $T_3$ states, respectively. These excitations are primarily single excitations from the highest occupied $\pi$ orbital to the lowest unoccupied valence $\pi^*$ orbital. Fig. 1 shows these results schematically. The uppermost row shows the result of the $\pi$-CI of Hay and Shavitt. The average error from the experimental values shown in the bottom row is 0.77 eV.

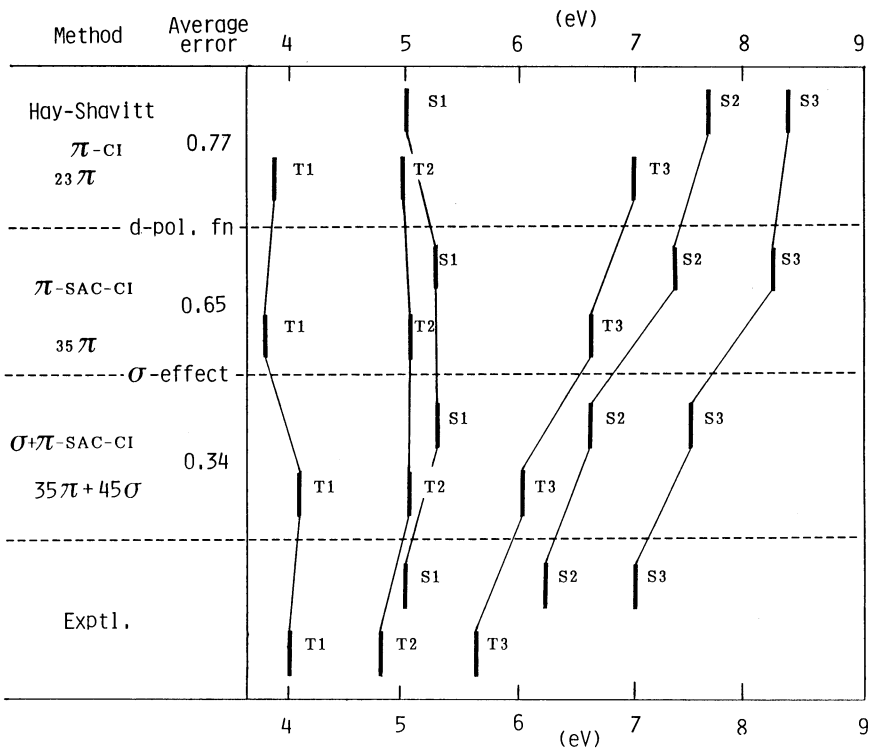


**Fig. 1.** Comparison of various levels of theoretical results with experiments for the valence $\pi \rightarrow \pi^*$ excitations of benzene

The second row shows the result of the SAC-CI calculation within $\pi$ MO's including $d$-polarization functions (basis $\neq 1$). The $d$ polarization function improves $T_3$ and $S_2$ states by 0.35 eV and 0.33 eV, respectively. The average error decreases to 0.65 eV. When we further relax the $\sigma$-electron space, the $T_3$, $S_2$, and $S_3$ states are much improved. The improvement is 0.63 eV for $T_3$, 0.71 eV for $S_2$ and 0.78 eV for $S_3$. The average error reduces to 0.34 eV. The remaining error still existing is in maximum 0.52 eV for the $S_3$ state. Thus, we conclude first that the $T_1$, $T_2$, and $S_1$ states are explainable within $\pi$-CI, second that for $T_3$ and $S_2$, the polarization $d_\pi$ function reduces the error by 0.3–0.4 eV and the $\sigma$-reorganization effect reduces the error by 0.6–0.7 eV, and third that for the $S_3$ state the effect of the $d_\pi$ polarization function is small, but the $\sigma$-reorganization effect is as large as 0.78 eV.

The $T_3$, $S_2$, and $S_3$ states are the so-called ionic V states of benzene [54]. It was conjectured that the $\sigma$-reorganization effect should be large for these states. The present result confirms this conjecture.

We observe some general trends in the reorganization of the $\sigma$ electrons due to the $\pi \rightarrow \pi^*$ excitations [6]. Since the $\pi \rightarrow \pi^*$ transition shifts the $\pi$ electrons to the outer rim of the hexagon, the $\sigma$ electrons on the other hand move into the inside of the hexagon. The reorganization is largest for the $S_3$ transition [6]. Table 2 shows the electronic part of the second moment for the ground and excited states of benzene. The axis $x$ is perpendicular to the plane and $y$ and $z$ lie on the plane. For the ground state the theory agrees well with experiment [55]. All the states shown here are genuine valence states except for the $S_3$ state. Within the $\pi$ SAC-CI, the $S_3$ state is relatively diffuse. It has the $\langle x^2 \rangle$ value twice as large as those of the other states. However, when the $\sigma$ MO space is relaxed, the state becomes very much compact. The $\langle x^2 \rangle$ value of the $\sigma + \pi$ calculation is only slightly larger than those of the other states. Therefore, the $S_3$ state is also a genuine valence state. This situation is very similar to the V state of ethylene. Huzinaga found a remarkable diffuseness of this state within

**Table 2.** Electronic part of the second moment of the valence excited states of benzene (a.u.)

| | SAC and SAC-CI | | | | | |
|---|---|---|---|---|---|---|
| | $35\pi$ | | | $35\pi + 45\sigma$ | | |
| State | $\langle x^2 \rangle$[a] | $\langle y^2 \rangle$ | $\langle z^2 \rangle$ | $\langle x^2 \rangle$ | $\langle y^2 \rangle$ | $\langle z^2 \rangle$ |
| $S_0$[b] | 30 | 215 | 215 | 31 | 215 | 215 |
| $S_1$ | 31 | 216 | 216 | 31 | 216 | 216 |
| $S_2$ | 34 | 219 | 219 | 33 | 217 | 217 |
| $S_3$ | 62 | 234 | 248 | 41 | 220 | 225 |
| $T_1$ | 30 | 216 | 216 | 31 | 216 | 216 |
| $T_2$ | 31 | 216 | 216 | 31 | 216 | 216 |
| $T_3$ | 32 | 217 | 217 | 32 | 217 | 217 |

[a] $x$ axis is perpendicular to the molecular plane.
[b] Experimental value [55]; $\langle x^2 \rangle = 28 \pm 6$, $\langle y^2 \rangle = \langle z^2 \rangle = 218 \pm 5$

$\pi$ calculation [56]. Tanaka observed that the $\sigma$ MO relaxation in CI worked to shrink the spatial extension of the V state [57]. Due to the more extensive CI [58-60] and SAC-CI [23] calculations, the $\langle x^2 \rangle$ value of the V state of ethylene is about twice as large as that of the ground state. This trend seems to be common to the relatively diffuse V states of the valence excited states of conjugated hydrocarbons.

In Fig. 2, we compare the SAC-CI results for the singlet Rydberg excitations with experiments [61]. This is the first systematic calculation of the Rydberg

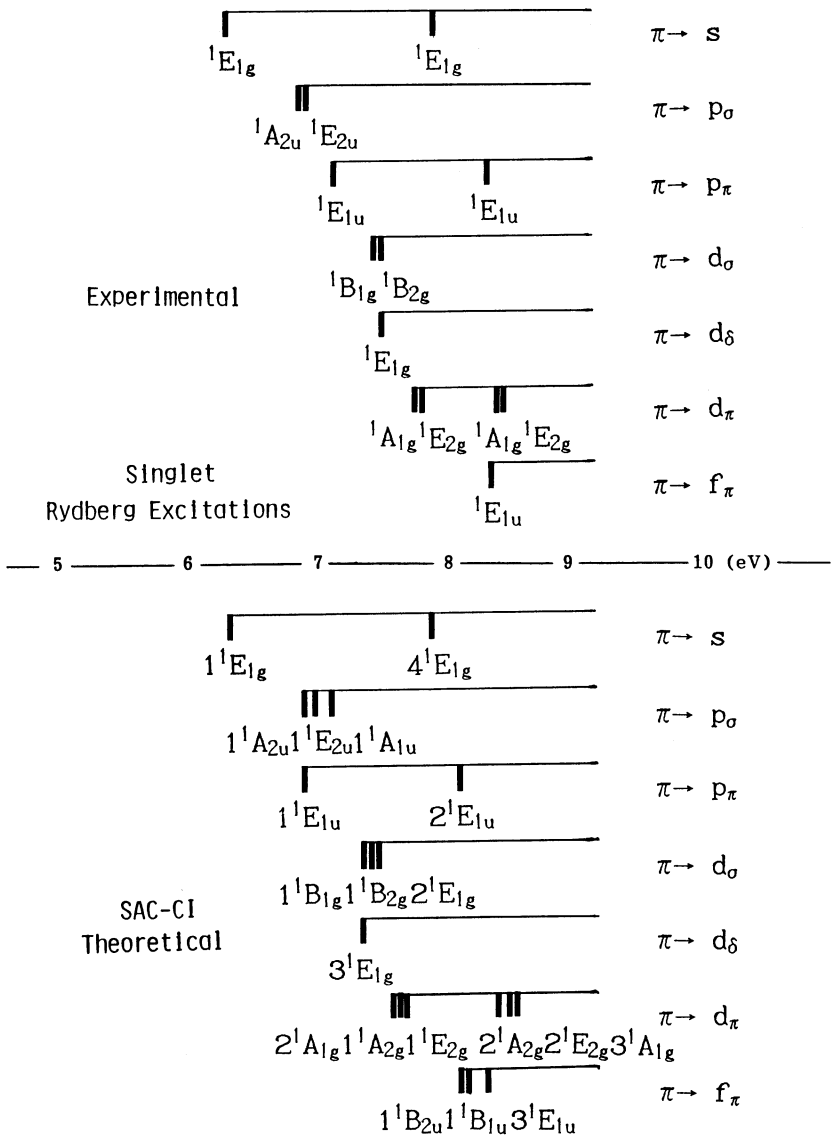


**Fig. 2.** Experimental (*above*) and theoretical (*below*) singlet Rydberg excitation energies of benzene

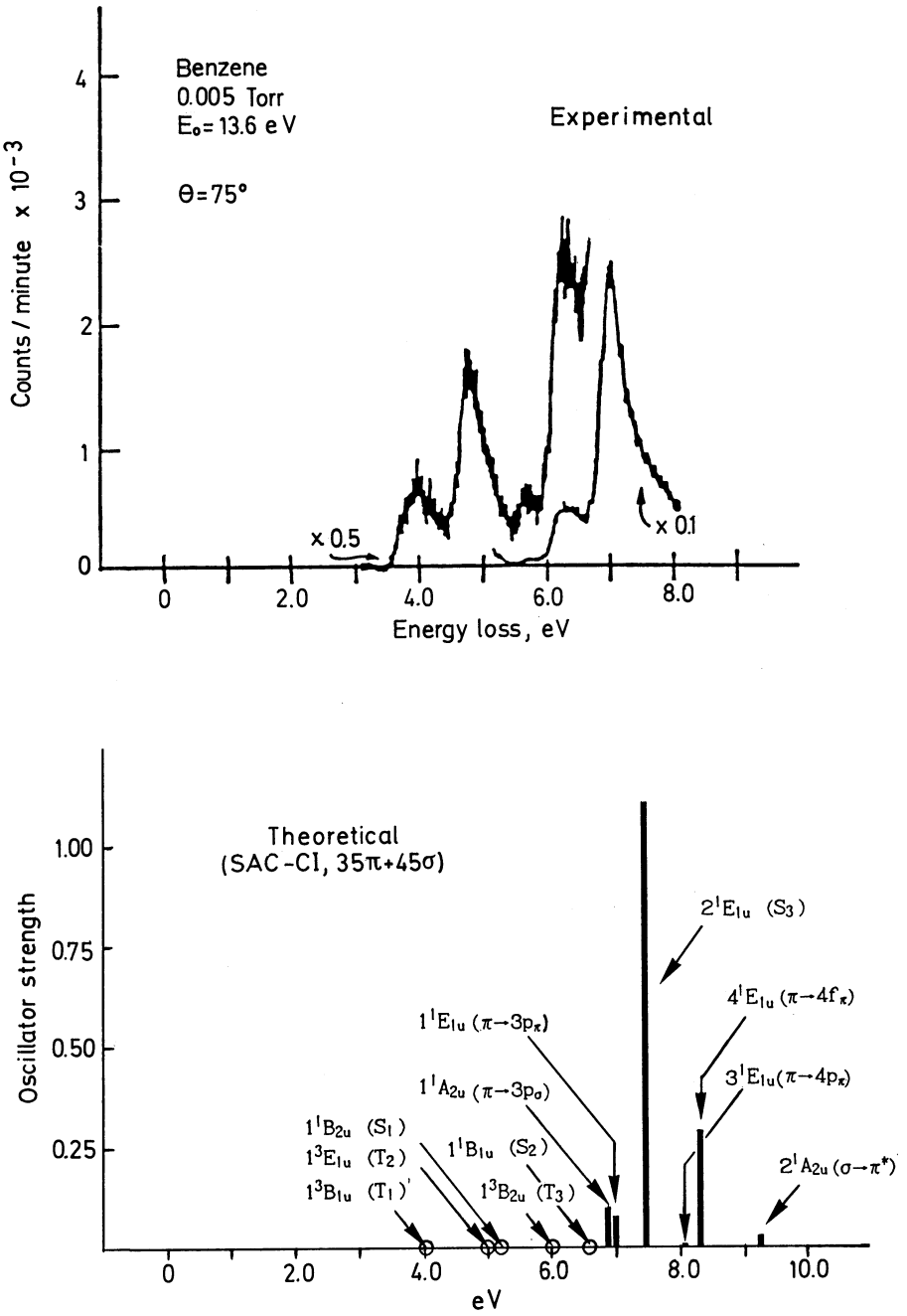


**Fig. 3.** Experimental (*above*) and theoretical (*below*) excitation spectra of benzene. The experimental spectra are due to Doering [53]

**Table 3.** Outer valence ionization potential of benzene

| State | Exptl. | SAC-CI eV (Δ)[a] | Green $f'n$[b] eV (Δ) | Koopmans' eV |
|---|---|---|---|---|
| $1^2E_{1g}\Pi$ | 9.3 | 8.88 (0.4) | 9.10 (0.2) | 9.26 |
| $2^2E_{2g}$ | 11.4 | 11.27 (0.1) | 11.95 (0.5) | 13.36 |
| $1^2A_{2u}\Pi$ | 12.1 | 12.41 (0.3) | 12.26 (0.2) | 13.73 |
| $1^2E_{1u}$ | 13.8 | 13.78 (0.0) | 14.46 (0.7) | 16.00 |
| $1^2B_{2u}$ | 14.7 | 14.22 (0.5) | 14.83 (0.1) | 16.83 |
| $1^2B_{1u}$ | 15.4 | 15.96 (0.5) | 15.75 (0.4) | 17.52 |
| $2^2A_{1g}$ | 16.9 | 16.91 (0.0) | 17.48 (0.6) | 19.39 |
| $1^2E_{2g}$ | 19.2 | 19.45 (0.2) | 20.01 (0.8) | 22.44 |

[a] Δ: difference from the experimental value [63]
[b] [62]

excitations of benzene involving both $\sigma$ and $\pi$ states. All the Rydberg excitations shown in Fig. 2 are from the $\pi$ orbital. The agreement between theory and experiment is excellent; viz., the theory reproduces the experimental values to within 0.2 eV. More details will be published elsewhere [6].

Fig. 3 shows a comparison of the SAC-CI theoretical spectra with the experimental one [53]. The peak at about 7 eV is the allowed transition and corresponds to the transition $S_0 \rightarrow S_3(^1E_{1u})$. By an enhancement of the shoulder below 6.8 eV, the spectrum in the 3–7 eV region was obtained. Several peaks observed there correspond to the transitions to the $S_1 \sim S_2$ and $T_1 \sim T_3$ states. In total, the agreement between theory and experiment is satisfactory.

In Table 3, we compare the ionization potentials of benzene calculated by the SAC-CI method with those calculated by the Green function method by von Niessen et al. [62] and with the experimental values [63]. This result is due to basis #1. Hirao and Kato [31] reported SAC-CI ionization potential of benzene using 4–31G basis set. The Green function method reproduces the experimental values to within 0.8 eV. The present SAC-CI calculation reproduces them to within 0.5 eV. Both theories show that between the higher two $\pi$ states ($^2E_{1g}$ and $^2A_{2u}$) there is a $\Sigma$ state ($2E_{2g}$), supporting the assignment due to Lindholm et al. [63] but against that of Potts et al. [64]. The Koopmans values give correct ordering, though they are not good quantitatively.

## 4. Exponentially generated wave functions

The SAC and SAC-CI theory is a very useful framework of the theory for studying ground, excited, ionized, and anion states of molecules [35]. We apply the SAC theory to the Hartree–Fock (HF) dominant state (usually the ground state) and generate excited, ionized, and anion states by the SAC-CI theory. Sometimes, the HF dominant state is not necessarily the ground state of the molecule [21, 27, 32].

However, when we study bond-breaking processes, for example, there occurs sometimes the situation in which the HF configuration is not at all dominant in

any lower lying states. The quasi-degenerate state is one such example. In such cases, the SAC theory is not at all appropriate, since it is a HF reference theory. We have to extend it to multireference version and more. Along this line, we have already published multireference (MR) SAC theory [4], and exponentially generated wave function (EGWF) theory [5] as a more general approach. In this section, we briefly review an outline of this theory.

### *4.1. Breakdown of the single reference theory*

We first analyse the source of the breakdown of the single reference theory [4]. We consider a model system in which only three configurations are important. They are $|0\rangle$, $S_I^\dagger|0\rangle$, and $S_I^{\dagger 2}|0\rangle$ with $|0\rangle$ and $S_I^\dagger$ being the HF configuration and an excitation operator, respectively. In an exact case, the wave function is written as

$$\Psi^e = |0\rangle + C_I S_I^\dagger|0\rangle + D_I S_I^{\dagger 2}|0\rangle. \tag{5}$$

The solution is straightforward and is given by

$$E = E_0 - \frac{|\langle 0|S_I H|0\rangle|^2}{\langle 0|S_I H S_I^\dagger|0\rangle - E - \dfrac{|\langle 0|S_I^2 H S_I^\dagger|0\rangle|^2}{\langle 0|S_I^2 H S_I^{\dagger 2}|0\rangle - E}} \tag{6}$$

where $E_0$ is the HF energy. In the cluster expansion theory, on the other hand, the coefficient of the product operator is a product of the coefficient of the lower-order term

$$\Psi^c = \exp(C_I S_I^\dagger)|0\rangle = |0\rangle + C_I S_I^\dagger|0\rangle + \tfrac{1}{2} C_I^2 S_I^{\dagger 2}|0\rangle. \tag{7}$$

The solution is obtained as

$$E = E_0 - \frac{|\langle 0|S_I H|0\rangle|^2}{\langle 0|S_I H S_I^\dagger|0\rangle - E - \dfrac{\langle 0|S_I H|0\rangle\langle 0|S_I H S_I^{\dagger 2}|0\rangle}{2\{\langle 0|S_I H S_I^\dagger|0\rangle + \frac{1}{2} C_I \langle 0|S_I H S_I^{\dagger 2}|0\rangle - E\}}}. \tag{8}$$

From Eqs. (6) and (8), we see that the cluster expansion theory simulates well the exact case when

1. the excitation energy to $S_I^{\dagger 2}|0\rangle$ is twice of that to $S_I^\dagger|0\rangle$, and
2. the matrix element satisfies the relation, $\langle 0|S_I H S_I^{\dagger 2}|0\rangle \simeq \langle 0|H S_I^\dagger|0\rangle$.
3. When $S_I^{\dagger 2}|0\rangle$ vanishes identically, two cases are trivially equal.

These relations would be satisfied if the electron correlations are separable, namely if only the dynamic correlations are important. However, when the operator $S_I^\dagger$ represents the internal correlation, the excitations among quasi-degenerate configurations, etc., these conditions will easily break down. When the product (coupling) of the two operators does not satisfy the above conditions 1-3, we call such coupling as "strong and synthetic coupling".

For example, let us consider a CO molecule at a large separation. In Fig. 4, we show a sketch of the electronic structure to help understanding. As an important

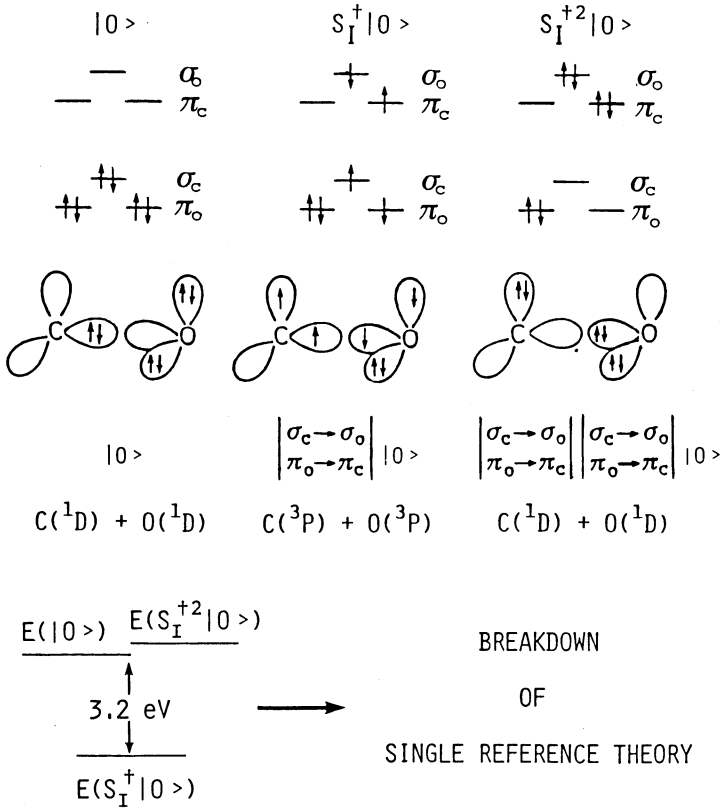


**Fig. 4.** Sketch of the electronic structure of the CO molecule at a large separation which shows the origin of the breakdown of the single reference theory

$S_I^\dagger$ operator we take a double excitation shown in Fig. 4, and therefore the operator $S_I^{\dagger 2}$ is the quadruple excitation. At a large separation, the configurations $|0\rangle$, $S_I^\dagger|0\rangle$, and $S_I^{\dagger 2}|0\rangle$ correspond respectively to the $^1D$, $^3P$ and $^1D$ states of carbon and oxygen. Therefore, the excitation energy from $|0\rangle$ to $S_I^\dagger|0\rangle$ is negative and that from $|0\rangle$ to $S_I^{\dagger 2}|0\rangle$ is almost zero. Thus, the condition 1 above completely breaks down and this leads to a breakdown of the single reference theory. Namely, the coupling of the two $S_I^\dagger$ operators here is not a "separable" coupling but a "strong and synthetic" coupling in the sense that it synthesizes an entirely new first-order state. Thus, the single reference cluster expansion theory breaks down for the CO molecule at a large separation.

Previously, we have shown the main configurations of the four $^1\Sigma$ states of the CO molecule with variations of the CO distance [4]. They were obtained by a full CI based on the HF orbitals. The HF configuration is dominant only near the equilibrium distance of the ground state. Single to quadruple excitations are also the main configurations of these four states, showing an interesting complexity which should be reproduced well by the advanced theory. A preliminary MR-SAC calculation has reproduced well these potential curves [4].

*4.2. Exponentially generated wave functions*

Now, I explain exponentially generated wave function (EGWF) theory [5]. We first define four exponential-type operators, three of which are new. They have been introduced to improve some restrictive features of an ordinary exponential operator.

$$\text{(I)}\quad \exp\left(\sum_K a_K A_K^\dagger\right) \equiv 1+\sum_K a_K A_K^\dagger+\frac{1}{2!}\sum_{K,L} a_K a_L A_K^\dagger A_L^\dagger + \frac{1}{3!}\sum_{K,L,M} a_K a_L a_M A_K^\dagger A_L^\dagger A_M^\dagger+\cdots, \tag{9}$$

$$\text{(II)}\quad \mathrm{EXP}\left(\sum_K a_K A_K^\dagger\right) \equiv a_0+\sum_K a_K A_K^\dagger+\frac{1}{2!}\sum_{K,L} a_K a_L A_K^\dagger A_L^\dagger + \frac{1}{3!}\sum_{K,L,M} a_K a_L a_M A_K^\dagger A_L^\dagger A_M^\dagger+\cdots, \tag{10}$$

$$\text{(III)}\quad \mathscr{exp}\left(\sum_K a_K A_K^\dagger\right) \equiv 1+\sum_K a_K A_K^\dagger+\frac{1}{2!}\sum_{K,L} a_{KL} A_K^\dagger A_L^\dagger + \frac{1}{3!}\sum_{K,L,M} a_{KLM} A_K^\dagger A_L^\dagger A_M^\dagger+\cdots, \tag{11}$$

$$\text{(IV)}\quad \mathscr{EXP}\left(\sum_K a_k A_K^\dagger\right) \equiv a_0+\sum_K a_K A_K^\dagger+\frac{1}{2!}\sum_{K,L} a_{KL} A_K^\dagger A_L^\dagger + \frac{1}{3!}\sum_{K,L,M} a_{KLM} A_K^\dagger A_L^\dagger A_M^\dagger+\cdots. \tag{12}$$

The first one is an ordinary exponential operator. In the capital EXP expansion, given by Eq. (10), the coefficient of the identity operator is a variable $a_0$ so that it can be small relative to the other terms. The variables are normalized within the linked terms. In the small script $\mathscr{exp}$ operator given by Eq. (11) and in the capital script $\mathscr{EXP}$ operator given by Eq. (12), the expansion is the same as those of the exp and EXP operators up to the linear terms. However, the coefficients of the product operators are not the products of the lower-order terms, but are the independent variables. Therefore, these operators can describe strong and synthetic coupling effect which is important in the region of quasi-degeneracy as explained above for the CO molecule.

The capital EXP operator is different from the ordinary exp operator. For a direct comparison, we renormalize the exp operator as

$$a_0 \exp\left(\sum_K a_K A_K^\dagger\right) = a_0+\sum_K a'_K A_K^\dagger+\frac{1}{2!}\frac{1}{a_0}\sum_{K,L} a'_K a'_L A_K^\dagger A_L^\dagger+\cdots \tag{13}$$

where $a'_K = a_0 a_K$. When $a_0$ is small, the unlinked terms of Eq. (13) tend to diverge. However, in the capital EXP operator given by Eq. (10), such divergence does not occur. Thus,

1. the EXP expansion behaves better when $a_0$ is small.

2. When $a_0$ is large, the difference of these two operators is small.
3. However, we note that the capital EXP operator is not multiplicative in the sense

$$\mathrm{EXP}\left(\sum_K a_K A_K^\dagger\right)\mathrm{EXP}\left(\sum_L b_L B_L^\dagger\right) \neq \mathrm{EXP}\left(\sum_K a_K A_K^\dagger + \sum_L b_L B_L^\dagger\right). \tag{14}$$

From the ordinary exponential operator, we obtain the SAC expansion.

$$\Psi^{\mathrm{SAC}} \equiv \exp\left(\sum_K a_K A_K^\dagger\right)|0\rangle. \tag{15}$$

This expansion is size-consistent because of the multiplicative character of the operator.

$$\exp\left(\sum_K a_K A_K^\dagger\right)\exp\left(\sum_L b_L B_L^\dagger\right) = \exp\left(\sum_K a_K A_K^\dagger + \sum_L b_L B_L^\dagger\right). \tag{16}$$

Further, because of this separability property, this expansion is suitable for a description of the dynamic correlation.

From the capital EXP operator, we obtain a new wave function, extended SAC (ESAC) wave function, defined by

$$\Psi^{\mathrm{ESAC}} \equiv \mathrm{EXP}\left(\sum_K a_K A_K^\dagger\right)|0\rangle. \tag{17}$$

This expansion is expected to behave better than the ordinary expansion in the region where $|0\rangle$ is less important. However, this expansion is not size-consistent, since the operator is not multiplicative.

From the script $\mathscr{exp}$ and $\mathscr{EXP}$ operators, we obtain a new wave function called exponentially generated CI (EGCI) wave function.

$$\Psi^{\mathrm{EGCI}} \equiv \mathscr{EXP}\left(\sum_K a_K A_K^\dagger\right)|0\rangle. \tag{18}$$

Though the $\mathscr{exp}$ and $\mathscr{EXP}$ operators are different in the coefficient of the identity operator, the two expansions are essentially the same, because all the coefficients involved are linearly independent. This wave function is a kind of a linear CI expansion, and yet is a straightforward generalization of the cluster expansion. Therefore, this expansion has the merits of both CI and cluster expansion theory, for example, an upper-bond nature and size consistency. This expansion is applicable to quasi-degenerate states and to both ground and excited states in all ranges of internuclear distance. However, a large defect of this expansion is that the dimension of the calculation becomes large. We have to borrow some advanced algorithms developed in the field of the CI calculations. Practically speaking, a general algorithm for the selection of the $A_K^\dagger$ operators and the truncation of the expansion will become important.

The methods of solutions of the SAC, ESAC, and EGCI wave functions are straightforward. We require Schrödinger equation $(H-E)|\Psi\rangle = 0$ in the space

of the linked configurations, $|0\rangle$ and $A_K^\dagger|0\rangle$ for the SAC and ESAC and $|0\rangle$, $A_K^\dagger|0\rangle$, $A_K^\dagger A_L^\dagger|0\rangle$, etc., for the EGCI. For the SAC and ESAC, this method gives a non-variational solution. For the EGCI, this method is also variational.

### *4.3. Multi-exponentially generated wave functions*

Here, we explain an idea of mixed- or multi-exponentially generated (MEG) wave functions. As already explained, the script $\mathscr{EXP}$ operator is very general and is suitable for quasi-degenerate correlation, for instance, but requires relatively large number of variables. The exp operator has some deficiency as already clarified but is suitable for a compact description of the dynamic correlation. Therefore, when a system involves two kinds of correlations, namely, quasi-degenerate correlation and dynamic correlation, we use the script $\mathscr{EXP}$ operator for the former and the ordinary exp operator for the latter. This mixed or multi use of different operators will permit an optimal use of the present idea both physically and practically. We call such wave functions as multi-exponentially generated (MEG) wave functions.

From two exponential-type operators, we obtain five MEG wave functions.

$$\Psi^{\mathrm{MEG1}} \equiv \mathrm{EXP}\left(\sum_K a_K A_K^\dagger\right) \mathrm{EXP}\left(\sum_L b_L B_L^\dagger\right)|0\rangle \tag{19}$$

$$\Psi^{\mathrm{MEG2}} \equiv \mathscr{EXP}\left(\sum_K a_K A_K^\dagger\right) \mathscr{EXP}\left(\sum_L b_L B_L^\dagger\right)|0\rangle \tag{20}$$

$$\Psi^{\mathrm{MEG3}} \equiv \exp\left(\sum_K a_K A_K^\dagger\right) \mathrm{EXP}\left(\sum_L b_L B_L^\dagger\right)|0\rangle \tag{21}$$

$$\Psi^{\mathrm{MEG4}} \equiv \exp\left(\sum_K a_K A_K^\dagger\right) \mathscr{EXP}\left(\sum_L b_L B_L^\dagger\right)|0\rangle \tag{22}$$

$$\Psi^{\mathrm{MEG5}} \equiv \mathrm{EXP}\left(\sum_K a_K A_K^\dagger\right) \mathscr{EXP}\left(\sum_L b_L B_L^\dagger\right)|0\rangle. \tag{23}$$

MEG1 and MEG2 include two same operators. We note that the two exp operators reduce to one because of the multiplicative property (Eq. (16)). However, the MEG2 wave function is not equal to the wave function,

$$\Psi^{\mathrm{EGCI}} = \mathscr{EXP}\left(\sum_K a_K A_K^\dagger + \sum_L b_L B_L^\dagger\right)|0\rangle.$$

In the former, two parts are assumed to be separable, but in the latter, the separability is not presumed. The wave functions MEG3 to MEG5 include different kinds of operators. Especially, the MEG4 wave function is equivalent to the MR-SAC wave function proposed previously [4]. In all of these wave functions, the operators involved are commutative. This is true for the MR-SAC (MEG4) theory even if the multireference part ($\mathscr{EXP}$ part) is not complete. This is in contrast to the previous multireference theories of Mukherjee et al. [11] and Jeziorski et al. [65].

Let us consider the MEG2 wave function. This wave function would be suitable for a description of two "separably" interacting quasidegenerate systems. However, when the two subsystems are large, part of the correlations would be classified into dynamic correlation, so that by introducing the wave function

$$\Psi^{\mathrm{MEG6}} \equiv \exp\left(\sum_K {}^d a_K \, {}^d A_K^\dagger\right) \mathscr{E}\mathscr{X}\mathscr{P}\left(\sum_K {}^q a_K \, {}^q A_K^\dagger\right) \times \exp\left(\sum_L {}^d b_L \, {}^d B_L^\dagger\right) \mathscr{E}\mathscr{X}\mathscr{P}\left(\sum_L {}^q b_L \, {}^q B_L^\dagger\right)|0\rangle$$
$$= \exp\left(\sum_K {}^d a_K \, {}^d A_K^\dagger + \sum_L {}^d b_L \, {}^d B_L^\dagger\right) \mathscr{E}\mathscr{X}\mathscr{P}\left(\sum_K {}^q a_K \, {}^q A_K^\dagger\right) \mathscr{E}\mathscr{X}\mathscr{P}\left(\sum_L {}^q b_L \, {}^q B_L^\dagger\right)|0\rangle, \tag{24}$$

we would be able to save the number of the variables without much affecting the accuracy. The superscripts $q$ and $d$ represent quasidegenerate and dynamic, respectively.

Now we consider the size consistency property. The capital EXP operator is not size consistent so that the MEG1, MEG3, and MEG5 wave functions are not size consistent, but the MEG2, MEG4, and MEG6 wave functions are size consistent.

## 5. Algorithm of calculation of the MEG4 wave function

Now, we consider the applications of the MEG4 theory [66]. We first explain the algorithm of the calculation of the MEG4 wave function

$$\Psi^{\mathrm{MEG4}} = \exp\left(\sum_I C_I S_I^\dagger\right) \mathscr{E}\mathscr{X}\mathscr{P}\left(\sum_K b_K M_K^\dagger\right)|0\rangle \tag{25}$$

where we adopt the symbols of the MR-SAC theory [4]. In the MEG4 wave function, the MR part $\mathscr{E}\mathscr{X}\mathscr{P}\,(\sum_K b_K M_K^\dagger)|0\rangle$ represents the zeroth-order description of the system, and the exp part represents the cluster expansion around the MR part. At a starting point, two different choices of the algorithm are possible. One is to consider the two sets of the operators $S_I^\dagger$ and $M_K^\dagger$ to be exclusive. We calculate the coefficients $C_I$ and $b_K$, iteratively. The other choice is to calculate the MR-part beforehand by a small EGCI calculation, and to consider the cluster expansion around this given function. The operators $S_I^\dagger$ and $M_K^\dagger$ need not be exclusive. In the present calculations, we adopt the first choice. Namely, the operators $M_K^\dagger$ and $S_I^\dagger$ are chosen exclusively.

The method of solution of the MEG4 wave function is straightforward. We require the Schrödinger equation within the main space under consideration, namely,

$$\langle 0|H - E|\Psi^{\mathrm{MEG4}}\rangle = 0, \tag{26a}$$
$$\langle 0|M_P(H - E)|\Psi^{\mathrm{MEG4}}\rangle = 0, \tag{26b}$$
$$\langle 0|M_P M_Q(H - E)|\Psi^{\mathrm{MEG4}}\rangle = 0, \tag{26c}$$
$$\langle \Phi_0|S_N(H - E)|\Psi^{\mathrm{MEG4}}\rangle = 0, \tag{26d}$$

where $\Phi_0$ is the main space of the MR part of Eq. (25). From the M-part equations, we obtain an eigenvalue equation

$$(\boldsymbol{A} - E\boldsymbol{S})\boldsymbol{b} = 0 \tag{27}$$

where the matrix $\boldsymbol{A}$ is non-symmetric and $\boldsymbol{S}$ is an overlap matrix. From Eq. (26d), we obtain a simultaneous linear equation

$$\boldsymbol{QC} = \boldsymbol{q}_0 \tag{28}$$

We solve these two equations iteratively and obtain the coefficients $\{b\}$, $\{C\}$ and the energy $E$.

We expand the M and S parts of the MEG4 wave function given by Eq. (25) up to the single product terms and obtain

$$\Psi^{\mathrm{MEG4}} = b_0|0\rangle + \sum_K b_K M_K^\dagger|0\rangle + \tfrac{1}{2}\sum_{KL} b_{KL} M_K^\dagger M_L^\dagger|0\rangle \tag{29a}$$

$$+ \sum_I b_I (\tfrac{1}{2} b_{KL}) M_I^\dagger M_K^\dagger M_L^\dagger|0\rangle + \tfrac{1}{2}\sum_{IJ}\sum_{KL} (\tfrac{1}{2} b_{IJ})(\tfrac{1}{2} b_{KL}) M_I^\dagger M_J^\dagger M_K^\dagger M_L^\dagger|0\rangle \tag{29b}$$

$$+ b_0 \sum_I C_I S_I^\dagger|0\rangle + \sum_K \sum_I b_K C_I S_I^\dagger M_K^\dagger|0\rangle + \tfrac{1}{2}\sum_{KL}\sum_I b_{KL} C_I S_I^\dagger M_K^\dagger M_L^\dagger|0\rangle \tag{29c}$$

$$+ \tfrac{1}{2} b_0 \sum_I \sum_J C_I C_J S_I^\dagger S_J^\dagger|0\rangle + \tfrac{1}{2}\sum_K \sum_I \sum_J b_K C_I C_J S_I^\dagger S_J^\dagger M_K^\dagger|0\rangle$$

$$+ \tfrac{1}{4}\sum_{KL}\sum_I \sum_J b_{KL} C_I C_J S_I^\dagger S_J^\dagger M_K^\dagger M_L^\dagger|0\rangle. \tag{29d}$$

Here the term (29a) is the zeroth order MR part. It gives a gross description of the system, say, more than 90% of the system. $M_K^\dagger$ are the operators necessary for the first description of the system. The product operators $M_K^\dagger M_L^\dagger$ describe the strong and synthetic coupling of the two operators. The term (29b) represents an unlinked approximation of the higher-order MR-part. The term (29c) is first order to the S-operators and the term (29d) is second order to the S-operators.

In the present calculations, the $M_K^\dagger$ operators are selected as those which are important in the preliminary singles and doubles (SD) CI. We form the product operators which are double, triple and quadruple excitations. The remaining single and double excitation operators are included in the $S_I^\dagger$ operators. We then generate the unlinked terms which are not redundant with the linked terms. When some $M_P^\dagger|0\rangle$ configuration is dominant ($b_K \simeq 1$), as in an ordinary excited state, the $S_I^\dagger$ operator acts actually as $S_I^\dagger M_P^\dagger$ as seen from Eq. (29). Therefore, in order to eliminate redundancy, we have to delete such $S_I^\dagger$ operator for which this product operator vanishes identically or is redundant with the other linked operators.

Figure 5 shows a flow chart of the program for the MEG4 calculations. We first do preliminary SD CI calculation and choose $M_K^\dagger$ and $S_I^\dagger$ operators and construct $M_K^\dagger M_L^\dagger$ operators. We include only linearly independent terms. Then, we carry out the EGCI calculation with these operators to obtain initial guess used below. We then calculate the integrals involving unlinked terms. We construct the

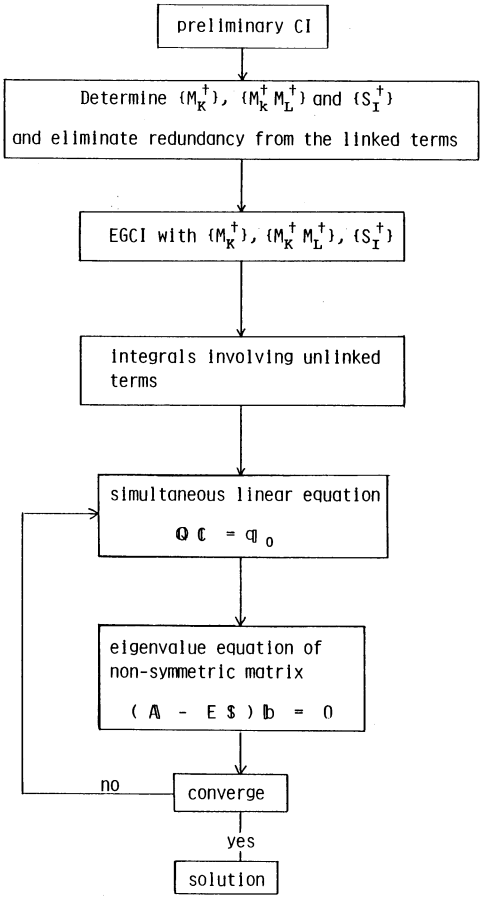


**Fig. 5.** Flow chart of the program for the MEG4 calculations

matrices $\boldsymbol{Q}$, $\boldsymbol{q}_0$, and $\boldsymbol{A}$ and solve Eqs. (28) and (27), iteratively until the convergence is obtained. In the present stage of the programming, I do not yet intend to introduce any special algorithms for rapid calculations. However, for the steps involving linear equation and diagonalization we found that FACOM VP 200, a Fujitsu super-computer, was very efficient. The calculation of the integrals involving unlinked terms is rather time-consuming. Probably, parallel processor would be very helpful for this step.

## 6. Applications of the MEG4 theory – calculation of potential energy curves

We test the present MEG4 theory and its algorithm by calculating the potential energy curves of some small molecules. First, we apply to the ground state of $F_2$. The basis set is the [4s2p] set of Huzinaga and Dunning [48]. The orbitals are calculated by the CAS-MC-SCF method [67] with $3 \times 1$ active orbitals. We use the program GAMESS [68] for the CAS-SCF and comparative CI calculations.

The active space for the MEG4 calculation consists of 9 orbitals occupied with 10 electrons.

Figure 6 shows the main configurations of the $F_2$ ground state in the full CI wave function. The lower figure along the potential curve shows the coefficient of the Hartree-Fock configuration and the upper one is the minus of that of the $\sigma \rightarrow \sigma^*$ doubly excited configuration. Near the equilibrium distance, the HF configuration is dominant but when the bond distance increases, the coefficient of the doubly excited configuration increases, and near 5 a.u., a quasidegenerate situation is realized.

Table 4 shows the ground state energy of $F_2$ at equilibrium [69] and elongated distances calculated by various levels of the CI and MEG4 methods. Values in

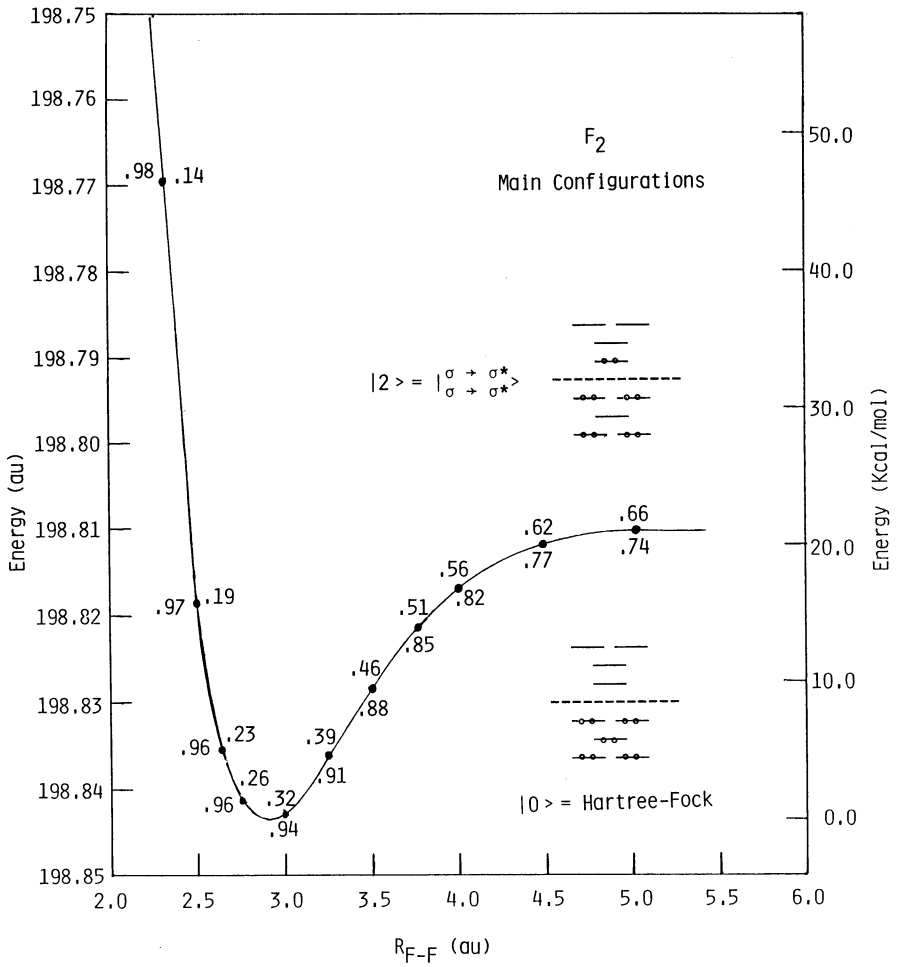


**Fig. 6.** Main configurations of the ground state of $F_2$ in the full CI wave function. The *lower figure* is the coefficient of the Hartree-Fock configuration and the *upper one* the minus of that of the $\sigma \rightarrow \sigma^*$ doubly excited configuration

**Table 4.** Ground state energy of $F_2$ calculated by various methods

| | $R = 2.66816$ a.u.[a] | | $R = 4.0$ a.u.[b] | |
|---|---|---|---|---|
| Method | Dimension | Energy (a.u.)[c] | Dimension | Energy (a.u.)[c] |
| Hartree-Fock | 1 | −198.70769 (81.30) | 1 | — |
| 3×1 CAS-SCF | 5 | −198.79072 (29.20) | 5 | −198.79216 (15.61) |
| SD-CI | 40 | −198.83258 (2.93) | 40 | −198.80827 (5.50) |
| SDT-CI | 146 | −198.83419 (1.92) | 146 | −198.81047 (4.12) |
| SDTQ-CI | 390 | −198.83714 (0.07) | 390 | −198.81689 (0.09) |
| full-CI | 726 | −198.83725 (0.00) | 726 | −198.81704 (0.00) |
| MEG4 | dim. (M, MM, S)[d] | | dim. (M, MM, S)[d] | |
| | 40 (2, 0, 38) | −198.83521 (1.28) | 40 (2, 0, 38) | −198.81446 (1.62) |
| | 44 (6, 4, 34) | −198.83628 (0.61) | 44 (8, 4, 32) | −198.81574 (0.82) |
| | 73 (12, 33, 28) | −198.83718 (0.04) | 85 (14, 45, 26) | −198.81596 (0.68) |
| | 102 (18, 62, 22) | −198.83684 (0.26) | 127 (22, 87, 18) | −198.81528 (1.10) |
| | 141 (22, 101, 18) | −198.83687 (0.24) | 159 (24, 119, 16) | −198.81561 (0.90) |

[a] At $R = 2.66816$ a.u., main configurations are $0.96|0\rangle - 0.23|2\rangle$

[b] At $R = 4.0$ a.u., main configurations are $0.82|0\rangle - 0.56|2\rangle$

[c] Figures in parentheses indicate energy difference in kcal $mol^{-1}$

[d] Dimensions of the M, MM, and S operators. The Hartree-Fock configuration is included in the M operator

parentheses are the energy differences in kcal $mol^{-1}$ from the full CI result. In the MEG4 calculation with the dimension 40, the reference is just two, namely the HF configuration and the doubly excited $\sigma\sigma^*$ configuration. Therefore, this is the two configuration reference SAC. The result is better than that of the SDT CI calculation of the dimension 146. When the product MM operators are included, the error reduces to one half with only an increase of 4 configurations. The best results are obtained at the dimension around 70–80, about one tenth of the dimension of the full CI. Further increase in dimension does not necessarily result in an improvement. This is because the higher-order contributions of the M-operators are not included by a truncation of the expansion. Further, an important observation here is that the dependence of the MEG4 result on the dimension of the calculation is quite small in comparison with that of the CI theory.

Figure 7 shows the potential energy curves of the $F_2$ molecule calculated by the CAS-MC-SCF, SD CI, SDT CI, MEG4, and full CI methods. The SDTQ CI results are close to the full CI one. The MEG4 curve is relatively close to the full CI curve. The difference is at most about 1 kcal $mol^{-1}$ near 5 a.u. Table 5 shows the bond length and dissociation energy of $F_2$ calculated by various methods. The result of MEG4 is close to the full CI one. The error in the dissociation energy is 0.6 kcal $mol^{-1}$.

We next apply the MEG4 method to the ground and excited states of LiF. The basis set is again due to Huzinaga and Dunning [48]. The orbitals are Hartree-Fock. The active space of the MEG4 calculation consists of 9 orbitals including 10 electrons.

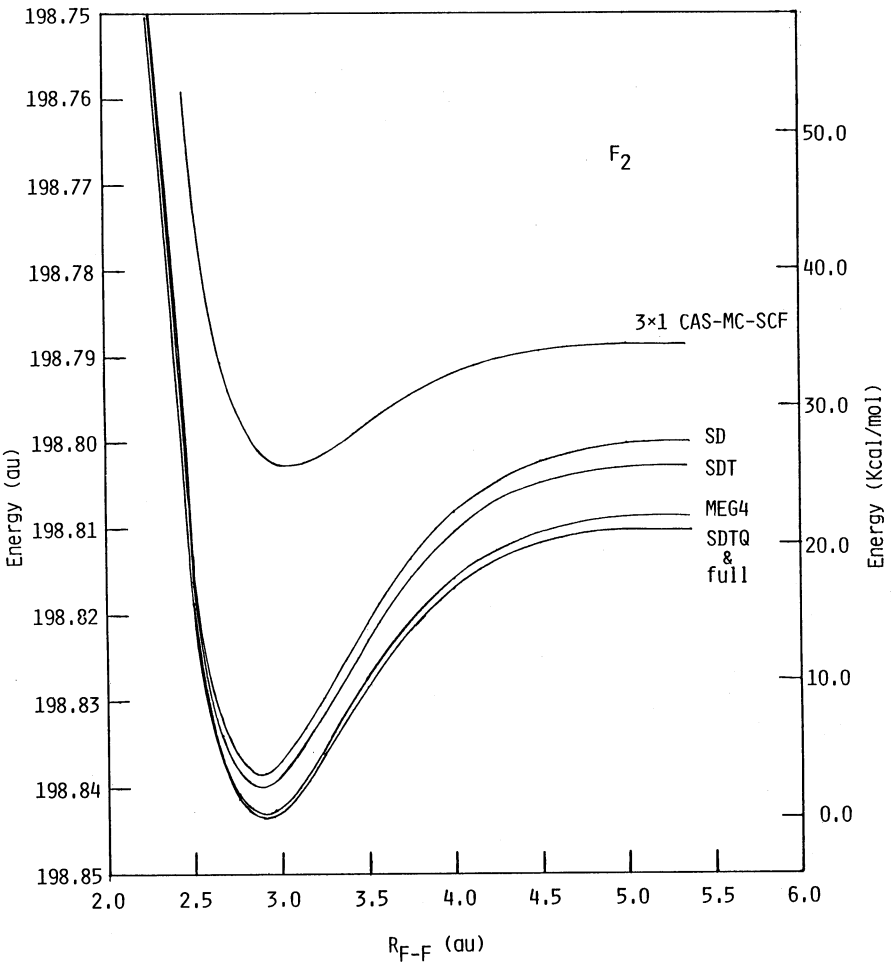


**Fig. 7.** Potential energy curve of $F_2$ calculated by CAS-SCF, CI, and MEG4 methods

**Table 5.** Bond length and dissociation energy of $F_2$ calculated by various methods

| Method | $R$ (a.u.) | $D_0$(kal mol$^{-1}$) |
|---|---|---|
| Exptl.[a] | 2.6682 | 36.945 |
| 3×1 CAS-SCF | 3.03 | 8.8 |
| SD-CI | 2.88 | 24.2 |
| SDT-CI | 2.89 | 23.5 |
| SDTQ-CI | 2.91 | 21.0 |
| full CI | 2.91 | 21.0 |
| MEG4 | 2.90 | 21.6 |

[a] [69]

For this system, the HF model is a very good approximation. For the ground state, the HF configuration is dominant. The lower three excited Σ states are typically singly excited states. They correspond to one-electron transfers from the $p_\sigma$ orbital of fluorine to the 2s orbital of Li, from the $p_\pi$ orbital of fluorine to the $p_\pi$ orbital of Li, and from the $p_\sigma$ orbital of fluorine to the $p_\sigma$ orbital of Li. In all of these excited states, the weight of the HF configuration is very small, so that the ordinary cluster expansion theory cannot be applicable to these excited states.

Table 6 shows the energies of the ground and excited states of LiF at $R = 4.0$ a.u. calculated by the CI and MEG4 methods. For the ground state, the SDT CI converges to the full CI, and for the excited states, the SDTQ CI converges to the full CI. The MEG4 result is the same as the full CI for the ground state. The MEG4 results are also excellent for the excited states. The differences from the full CI are only few per cents of a millihartree. In contrast to this, the single reference SAC theory do not give a convergence for these excited states, though it gives a reasonable value for the ground state. Fig. 8 shows the potential energy curves of the ground and excited states of LiF. The MEG4 curves overlap almost completely the full CI curves for both the ground and excited states. Thus, we conclude that the MEG4 theory is applicable not only to the ground state but also to the excited states.

We next apply the MEG4 theory to the ground and excited states of the CO molecule. This system gives a good test for the multireference type theory, because the main configurations of the ground and excited states change drastically as the CO distance increases [4]. The basis set is again the [4s2p] set of Huzinaga and Dunning [48]. The orbitals are Hartree-Fock. The active space consists of ten orbitals occupied by six electrons. In the present MEG4 calculation, we don't include the term b of Eq. (29) since in the M and MM operators we include the terms only up to quadruple excitations. This is insufficient for the CO molecule at larger separations. In this sense, the present result is preliminary in nature.

Fig. 9 shows the main configurations of the first three $^1\Sigma$ states of the CO molecule in the full CI. As shown previously in the minimal STO-6G basis calculation [4],

**Table 6.** Ground and excited states of LiF at $R = 4.0$ a.u. calculated by various methods

| Method | Dimension | Ground $X\,^1\Sigma$ | Excited state | | |
|---|---|---|---|---|---|
| | | | $p_\sigma(F) \rightarrow 2s(Li)$ | $p_\pi(F) \rightarrow p_\pi(Li)$ | $p_\sigma(F) \rightarrow p_\sigma(Li)$ |
| Hartree-Fock | 1 | −106.921495 | — | — | — |
| SD-CI | 71 | −106.921850 | −106.698065 | −106.624220 | −106.588245 |
| SDT-CI | 298 | −106.921862 | −106.698307 | −106.624653 | −106.588437 |
| SDTQ-CI | 751 | −106.921862 | −106.698308 | −106.624655 | −106.588438 |
| Full-CI | 1436 | −106.921862 | −106.698308 | −106.624655 | −106.588438 |
| MEG4 | 80–180 | −106.921862 | −106.698298 | −106.624610 | −106.588422 |
| (Difference from full CI) | | (0.000000) | (0.000010) | (0.000045) | (0.000016) |
| SAC | 71 | −106.921855 | non-converge | non-converge | non-converge |

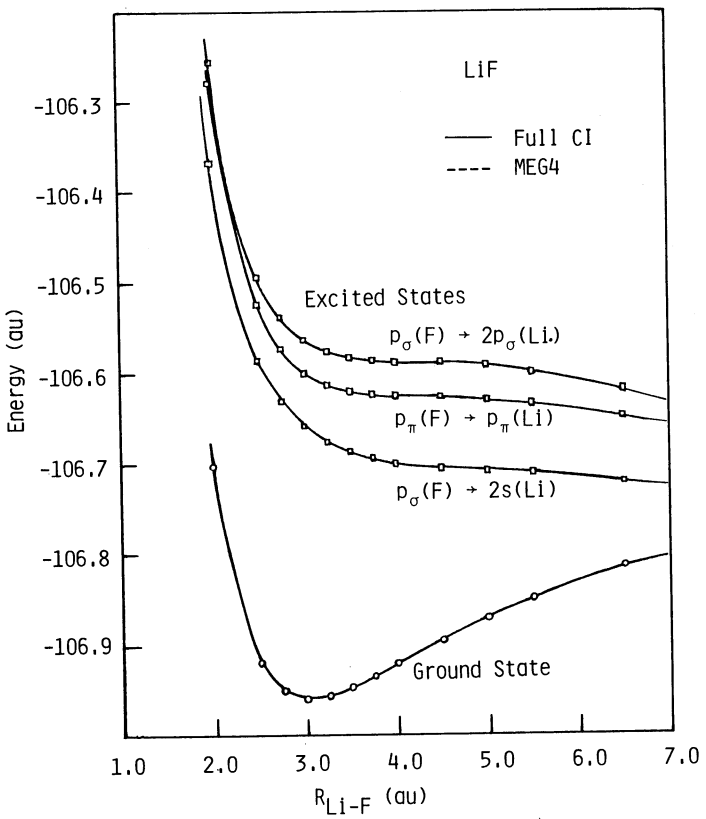


**Fig. 8.** Potential energy curves of the ground and excited states of LiF calculated by the MEG4 and full CI methods

the main configurations change drastically as the CO distance increases. Though the HF configuration is dominant near the equilibrium geometry of the ground state, its weight decreases monotonously, the single $\pi \rightarrow \pi^*$ excitation mixes in the intermediate region, and finally, the double excitation from $\pi$ to $\pi^*$ and from $n$ to $\sigma^*$ becomes a dominant configuration near the dissociation limit. The second state is a $n \rightarrow \sigma^*$ Rydberg type excited state at a short distance, but suffers avoided crossing near 2.2 a.u. and becomes then singly excited $\pi \rightarrow \pi^*$ state. When the CO bond is elongated further the HF configuration mixes. Namely, the avoided crossing occurs among the three states. Afterwards, triply and quadruply excited configurations increase and the state dissociates into the $^3P$ states of carbon and oxygen. The third state is a $\pi \rightarrow \pi^*$ excited state at short distance but becomes $n \rightarrow \sigma^*$ excited state at a longer distance by an avoided crossing. Then, doubly excited $\pi \rightarrow \pi^*$ configuration becomes main and finally the HF configuration becomes main and the state dissociates into the $^1$D states of carbon and oxygen. Thus, the character of the electronic structure of the CO molecule changes drastically as the CO distance increases.

In Fig. 10 we compare the MEG4 (broken line) and full CI (real line) potential

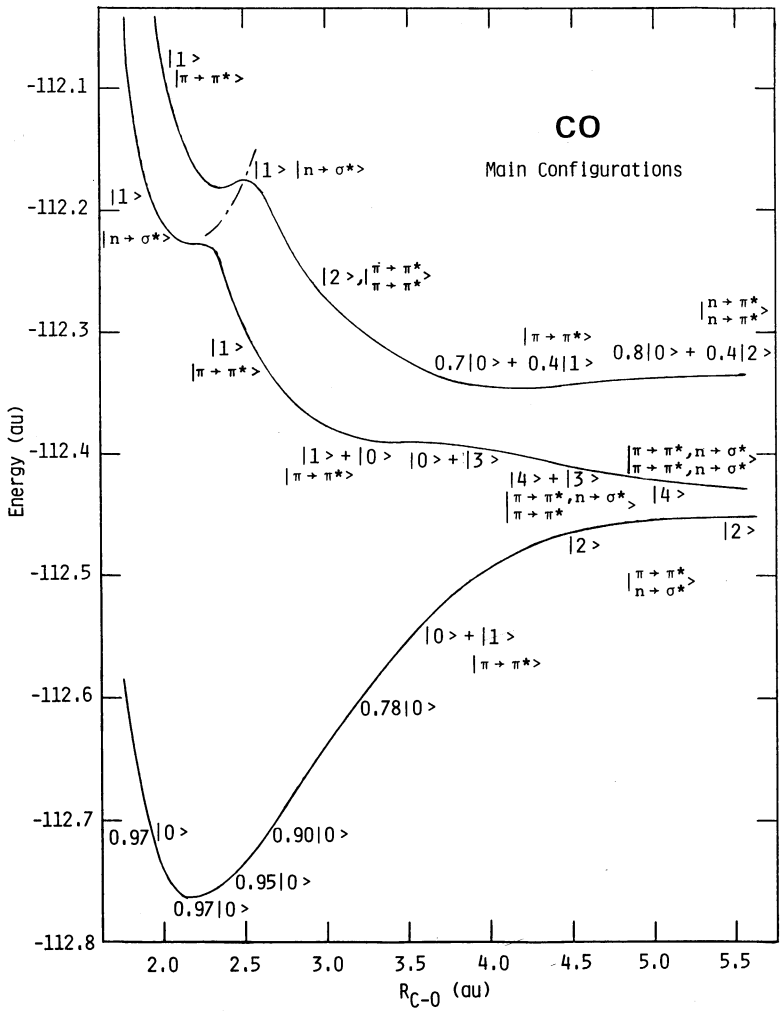


**Fig. 9.** Main configurations in the full CI of the ground and excited $^1\Sigma$ states of the CO molecule based on the Hartree-Fock orbitals

curves for the ground and excited states of the CO molecule. In all of the regions, the MEG4 curves reproduce reasonably well the full CI curves. Near the 3-4 a.u. region of the second excited state, the discrepancy is relatively large, because of a complex multireference nature of the wave function as shown in Fig. 9.

The last example of the applications is the ground state of water at equilibrium and elongated distances. Some years ago, full CI calculations were reported for water at equilibrium and two elongated distances within the full [4s2p] active space [70]. Some related studies have also been published [17, 71-73]. We carry out here the test calculations to see the effectiveness of the present theory. The orbitals we used are the CAS-SCF orbitals within $3 \times 3$ active space. At $R = 1.5$ Re,

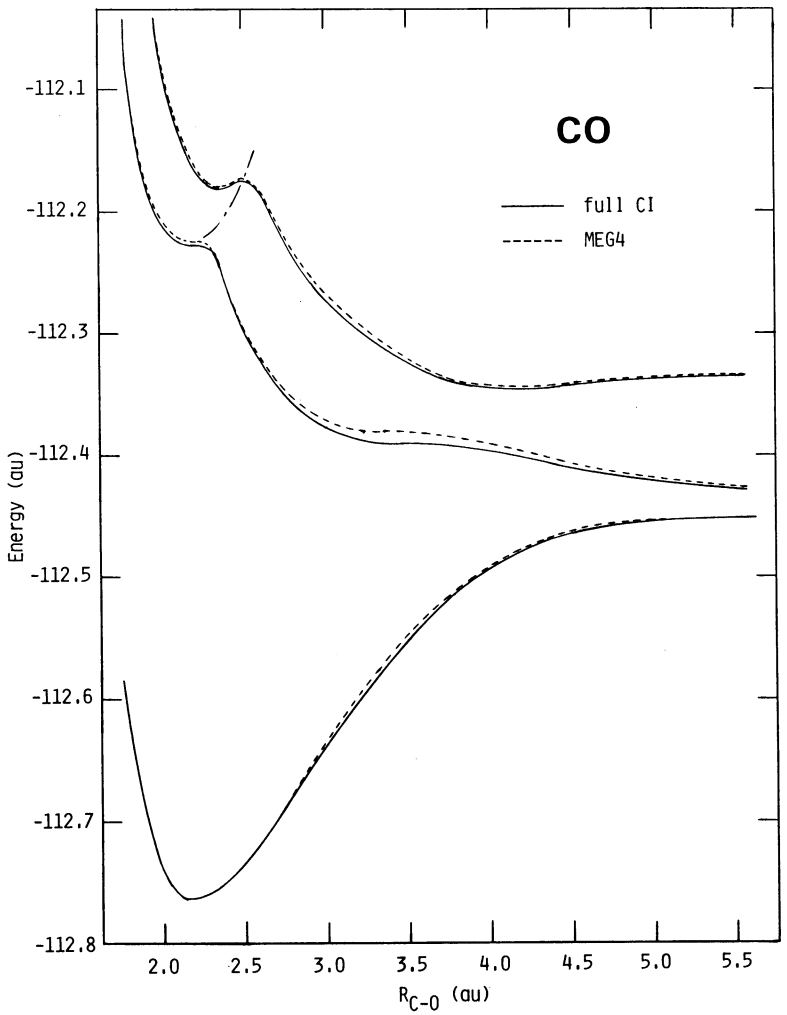


**Fig. 10.** MEG4 and full CI potential energy curves of the ground and excited $^1\Sigma$ states of the CO molecule based on the [4s2p] basis set

we choose as the M operators 5 single and 26 double excitation operators. From these M operators, 56 triple and 113 quadruple excitations are generated. Other single and double excitation operators are grouped into the S operators. The total dimension is 527. For the other distances, the construction of the M and S operators is similar. The total dimension is 736 for $R$ = Re and 1140 for $R$ = 2.0 Re.

In Table 7, we compare the dimensions and the correlation energies of the double-zeta $H_2O$ calculated by the various levels of the CI method, the MEG4 method and the SAC method. The value in parentheses shows the percentage of the correlation energy calculated. The CI method is slowly convergent: the dimension is 3203 for the SDT CI, 17 678 for the SDTQ CI and 256 473 for the

**Table 7.** Dimensions and correlation energies of the various methods for double-zeta $H_2O$ (a.u.)

| | $R$ = Re | | $R$ = 1.5 Re | | $R$ = 2.0 Re | |
|---|---|---|---|---|---|---|
| | Dimension | $E_{corr}$ (%) | Dimension | $E_{corr}$ (%) | Dimension | $E_{corr}$ (%) |
| Hartree-Fock[a] | 1 | 0.0 | 1 | 0.0 | 1 | 0.0 |
| SD-CI[b] | 361 | −0.14018 (94.7) | 361 | −0.18861 (89.4) | 361 | −0.24964 (80.5) |
| SDT-CI[b] | 3 203 | −0.14132 (95.5) | 3 203 | −0.19231 (91.2) | 3 203 | −0.26035 (84.0) |
| SDTQ-CI[b] | 17 678 | −0.14776 (99.8) | 17 678 | −0.20989 (99.5) | 17 678 | −0.30572 (98.6) |
| full-CI[b] | 256 473 | −0.14803 (100.0) | 256 473 | −0.21099 (100.0) | 256 473 | −0.31007 (100.0) |
| MEG4 | 736 | −0.14712 (99.4) | 527 | −0.20992 (99.5) | 1 140 | −0.30901 (99.7) |
| SAC[c] | 361 | −0.14642 (98.9) | 361 | −0.20511 (97.2) | 361 | −0.29524 (95.2) |

[a] Hartree-Fock energy is −76.00984 a.u., −75.80353 a.u., and −75.59518 a.u. for $R$ = Re, $R$ = 1.5 Re, and $R$ = 2.0 Re, respectively.
[b] [70]
[c] [17]

full CI. The MEG4 method is more rapidly convergent: the dimension is as small as 500–1200. The correlation energy calculated by the MEG4 method is about 99.5% of the full CI for all the distances. In other theories, the error increases at larger separations. For the SAC method, the dimension is 361, the same as that of the SD CI, but the energy error increases with increasing OH distance because of the decreasing weight of the HF configuration.

Fig. 11 shows the plots of the energy errors relative to the full CI for different OH distances. The multireference (MR) CI results are due to Brown et al. [72] and the result of the multireference linearized coupled cluster method (MR-LCCM) is due to Laidig et al. [73]. The values in parentheses are the dimensions of the calculations. The energy error increases rapidly in the smaller dimension CI and MR-CI, MBPT (many body perturbation theory) [71], CCSD (coupled cluster singles and doubles) [71] and SAC method [17]. The latter two are equivalent for the closed-shell non-variational case. In the larger MR-CI calculations, the dependence becomes flat, but the dimension is larger than 7906. The result of the present MEG4 theory is given by a bold line. The dependence is flat even though the dimension is very small. This is the result of the multi use of the exponential-type operators in the MEG4 theory. The energy error is about 1 millihartree, everywhere.

From the applications of the MEG4 theory shown in this section, we may conclude that the MEG4 theory gives reliable results not only for ground states but also for excited states and quasi-degenerate states.

## 7. Summary and conclusion

We summarize the SAC-CI study of benzene as follows.

1. We performed $\pi + \sigma$ SAC and SAC-CI calculations of the ground and excited states of benzene using a large active space. Both valence and Rydberg excitations and ionizations were studied.

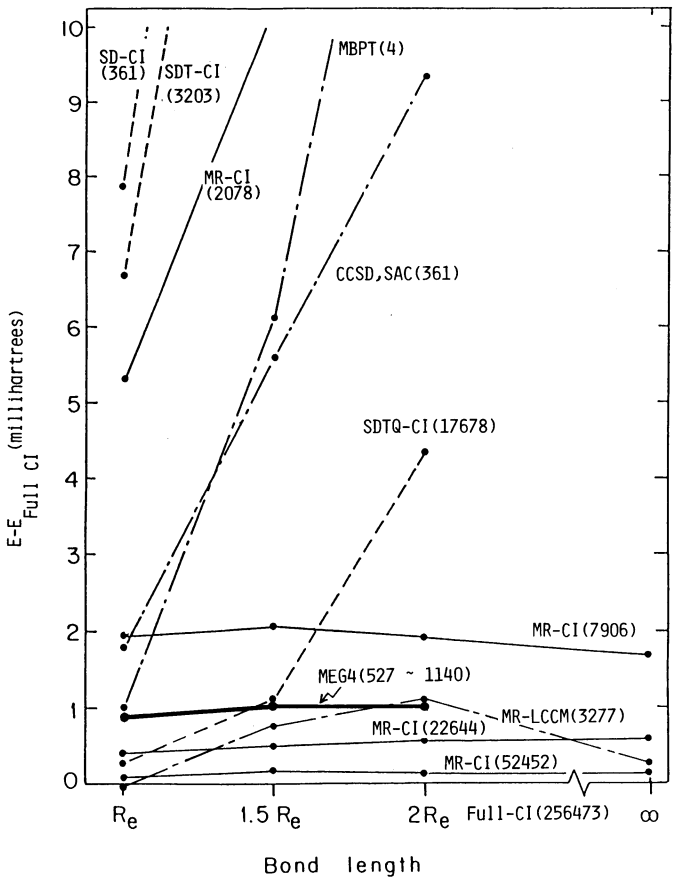


**Fig. 11.** Energy errors relative to the full CI for the double-zeta $H_2O$. (Values in parentheses show the dimensions of the variables)

2. For the valence $\pi \rightarrow \pi^*$ excitations, we observed that the $T_1$, $T_2$, and $S_1$ states are understood within only $\pi$-space. For the $T_3$, $S_2$, and $S_3$ states, the so-called V states, the effect of the reorganization of the $\sigma$ electrons was very large. They are 0.63, 0.71, and 0.78 eV, respectively. For the $T_3$ and $S_2$ states, the polarization $d_\pi$ functions on carbons were also important and improved by 0.35 and 0.33 eV, respectively. The average error reduced from 0.78 eV of the $\pi$ CI due to Hay and Shavitt [45] to 0.34 eV of the present result.

3. We first performed a systematic calculation of the Rydberg excited states involving both $\sigma$ and $\pi$ states. The theory reproduced the experimental value to within 0.2 eV.

4. The SAC-CI ionization potential reproduced the experimental value to within 0.5 eV.

We summarize the approach of the exponentially generated wave function (EGWF) theory as follows.

1. The idea of the exponentially generated wave function theory was explained in [5]. We introduced some strange exponential operators, capital EXP, script $\mathcal{exp}$ and script capital $\mathscr{EXP}$ operators in Eqs. (10)-(12). With these operators, We defined the new wave functions, the extended SAC (ESAC) wave function given by Eq. (17) and the exponentially generated CI (EGCI) wave function given by Eq. (18). Then, by a mixed or multi use of these operators, We introduced several MEG (multi-exponentially generated) wave functions. Such mixed use of the operators permits an optimal theory of electron correlations both physically and practically. For example, the MEG4 wave function defined in this way is identical with the MR-SAC wave function previously introduced [4].

2. The present algorithm for the applications of the MEG4 theory was tested. A potential utility of the theory was shown from the applications to the potential energy curves of the ground states, quasi-degenerate states, and excited states of some small diatomics and triatomics.

*Acknowledgement.* The author thanks Drs. S. Huzinaga and M. Klobukowski for inviting him to the Symposium on Computational Quantum Chemistry and Parallel Processors where he contributed this presentation. Mr. O. Kitao is the coworker on the SAC-CI study of the excited states of benzene. The full CI and higher order CI calculations used for comparisons in Sect. 6 were carried out using the Program GAMESS [68]. I thank the authors of this nice program. I thank Messrs. Y. Matsuzaki, T. Nakao, and M. Komori for some assistance in the reference CI calculations.

## References

1. Nakatsuji H, Hirao K (1978) J Chem Phys 68:2053
2. Nakatsuji H (1978) Chem Phys Lett 59:362
3. Nakatsuji H (1979) Chem Phys Lett 67: 329, 334
4. Nakatsuji H (1985) J Chem Phys 83:713; see also Nakatsuji H, Hada M (1986) In: Smith VH, Schaefer HF, Morokuma K (eds) Applied quantum chemistry, p 93, New York, Reidel
5. Nakatsuji H (1985) J Chem Phys 83:5743
6. Kitao O, Nakatsuji H: to be submitted
7. Coester F (1958) Nucl Phys 7:421; Coester F, Kümmel H (1960) Nucl Phys 17:477
8. Sinanoglu O (1962) J Chem Phys 36:706, 3198; (1964) Adv Chem Phys 6:315
9. Primas H (1965) In: Sinanoglu O (ed) Modern quantum chemistry, vol II, p 45. New York, Academic Press
10. Cizek J (1966) J Chem Phys 45:4256; Cizek J (1969) Adv Chem Phys 14:35; Paldus J, Cizek J, Shavitt I (1972) Phys Rev A5:50; Paldus J (1983) In: Lödwin P-O, Pullman B (eds) New horizons of quantum chemistry, p 183. Dordrecht, Reidel
11. Mukherjee D, Moitra RK, Mukhopadhyay A (1975) Mol Phys 30:1861; (1977) 33:955
12. Bartlett RJ (1981) Annu Rev Phys Chem 32:359
13. Thouless DJ (1960) Nucl Phys 21:225
14. Nakatsuji H (1973) J Chem Phys 59:2586
15. Nakatsuji H, Hirao K (1977) Chem Phys Lett 47:569; (1978) J Chem Phys 68:4279
16. Nakatsuji H, Hirao K (1981) Int J Quantum Chem 20:1301
17. Hirao K, Hatano T (1983) Chem Phys Lett 100:519; (1984) 111:533
18. Hirao K, Nakatsuji H (1981) Chem Phys Lett 79:292
19. Nakatsuji H, Ohta K, Hirao K (1981) J Chem Phys 75:2952
20. Nakatsuji H (1983) Chem Phys 75:425
21. Nakatsuji H (1983) Int J Quantum Chem S17:241
22. Hirao K (1983) J Chem Phys 79:5000

23. Nakatsuji H (1984) J Chem Phys 80:3703
24. Hirao K (1984) J Am Chem Soc 106:6283
25. Nakatsuji H, Kitao O, Yonezawa T (1985) J Chem Phys 83:723
26. Nakatsuji H, Ushio J, Yonezawa T (1985) Can J Chem 63:1857
27. Kitao O, Nakatsuji H (1986) Proc Ind Acad Sci 96:155
28. Nakatsuji H, Hada M (1985) J Am Chem Soc 107:8264
29. Nakatsuji H, Yonezawa T (1982) Chem Phys Lett 87:426
30. Nakatsuji H (1983) Chem Phys 76:283
31. Hirao K, Kato H (1983) Chem Phys Lett 98:340
32. Nakatsuji H, Ohta K, Yonezawa T (1983) J Phys Chem 87:3068
33. Hirao K, Nakatsuji H (1978) J Chem Phys 69:4548
34. Ohta K, Nakatsuji H, Hirao K, Yonezawa T (1980) J Chem Phys 73:1770
35. (a) Nakatsuji H (1985) Program system for SAC and SAC-CI calculations. Program Library No. 146 (Y4/SAC). Data Processing Center of Kyoto University
(b) Nakatsuji H (1986) Program Library SAC85 (No 1396), Computer Center of the Institute for Molecular Science, Okazaki, Japan
36. Hückel E (1931) Z Phys 70:206; (1931) 72:310; (1932) 76:628
37. Pauling L, Wheland GW (1933) J Chem Phys 1:362; (1934) 2:484
38. Goeppert-Mayer M, Sklar AL (1938) J Chem Phys 6:645
39. Pariser R, Parr RG (1953) J Chem Phys 21:466; (1953) 21:767
40. Pople JA (1953) Trans Faraday Soc 49:1375
41. Ohno K, Noro T (1986) In: Higuchi J (ed) Molecular electronic structure, p 83. Tokyo, Kyoritsu (in Japanese)
42. Buenker RJ, Whitten JL, Petke JD (1968) J Chem Phys 49:2261
43. Peyerimhoff SD, Buenker RJ (1970) Theor Chim Acta 19:1
44. Rose JB, Shibuya T, McKoy V (1974) J Chem Phys 60:2700
45. Hay PJ, Shavitt I (1973) Chem Phys Lett 22:33; (1974) J Chem Phys 60:2865
46. Rancural R, Huron B, Praud L, Malrieu PJ, Berthier G (1976) J Mol Spectrosc 60:259
47. Langseth A, Stoicheff BP (1956) Can J Phys 34:350
48. Huzinaga S (1965) J Chem Phys 42:1293; Dunning TH Jr (1970) J Chem Phys 53:2823
49. Dunning TH Jr, Hay PJ (1977) In: Schaefer HF (ed) Modern theoretical chemistry. New York, Plenum
50. Bender CF (1972) J Compt Phys 9:547
51. Yoshimine M (1978) In: Moler C, Shavitt I. (eds) Report on the workshop: Numerical algorithms in chemistry: Algebraic methods, p 142. Lawrence Berkeley Lab, University of California
52. King HF, Dupuis M, Rys J (1979) Program Library HONDOG (No 343), Computer Center of the Institute for Molecular Science, Okazaki, Japan
53. Lassettre EN, Skerbele A, Dillon MA, Ross KJ (1968) J Chem Phys 48:5066; Doering J (1969) J Chem Phys 51:2866
54. Mulliken RS (1974) Chem Phys Lett 25:305; Iwata S, Freed KF (1974) J Chem Phys 61:1500
55. Schoemaker RL, Flygare WH (1969) J Chem Phys 51:2988
56. Huzinaga S (1962) J Chem Phys 36:453
57. Tanaka K (1972) Int J Quantum Chem 6:1087
58. McMurchie LE, Davidson ER (1977) J Chem Phys 66:2959; (1977) 67:5613
59. Brooks BR, Schaefer, HF (1978) J Chem Phys 68:4839
60. Buenker RJ, Peyerimhoff SD, Shih S-K (1980) Chem Phys Lett 69:7
61. Wilkinson PG (1956) Can J Phys 34:596; Johnson PM (1976) J Chem Phys 64:4143; Whetten RL, Grubb SG, Otis CE, Albrecht AC, Grant ER (1985) J Chem Phys 82:1115; Grubb SG, Otis CE, Whetten RL, Grant ER, Albrecht AC (1985) J Chem Phys 82:1135
62. Von Niessen W, Cederbaum LS, Kraemer WP (1976) J Chem Phys 65:1378; Cederbaum LS, Domcke W, Schirmer J, Von Niessen W, Diercksen GHF, Kraemer WP (1978) J Chem Phys 69:1591
63. Jonsson B-Ö, Lindholm E (1969) Ark Fys 39:65; Fridh C, Asbrink L, Lindholm E (1972) Chem Phys Lett 15:282
64. Potts AW, Price WC, Streets DG, Williams TA (1972) Faraday Disc Chem Soc 54:168

65. Jeziorski B, Monkhorst HJ (1981) Phys Rev A24:1668
66. Nakatsuji H: to be published
67. Siegbahn P, Heiberg A, Roos B, Levy B (1980) Phys Scrip 21:323
68. Brooks BR, Saxe P, Laidig WD, Dupuis M (1981) Program Library GAMESS (No 481), Computer Center of the Institute for Molecular Science, Okazaki, Japan
69. Huber KP, Herzberg G (1979) Molecular spectra and molecular structure. IV. Constants of diatomic molecules. New York, Van Nostrant Reinhold
70. Saxe P, Schaefer III HF, Handy NC (1981) Chem Phys Lett 79:202; Harrison RJ, Handy NC (1983) Chem Phys Lett 95:386
71. Bartlett RJ, Sekino H, Purvis III GD (1983) Chem Phys Lett 98:66
72. Brown FB, Shavitt I, Shepard R (1984) Chem Phys Lett 105:386
73. Laidig WD, Bartlett RJ (1984) Chem Phys Lett 104:424